A Simple Electromagnetically Fed Circularly-Polarized Circular Microstrip Antenna

Mursyidul I. Sabran [1], Sharul Kamal A. Rahim [1], Ping Jack Soh [2], Chee Y. Leow [1], and Guy A. E. Vandenbosch [3]

[1] Wireless Communication Centre (WCC), Faculty of Electrical Engineering
Universiti Teknologi Malaysia, UTM Skudai, 81310, Johor, Malaysia
mursyid@fkegraduate.utm.my, sharulkamal@fke.utm.my, bruceloew@fke.utm.my

[2] The Advanced Communication (ACE) Centre of Excellence, School of Computer and Communication Eng.
Universiti Malaysia Perlis (UniMAP), 02600 Arau, Perlis, Malaysia
pjsoh@unimap.edu.my

[3] ESAT-TELEMIC Research Div.
KU Leuven, Kasteelpark Arenberg 10, 3001 Leuven, Belgium
guy.vandenbosch@esat.kuleuven.be

Abstract ─ Existing literature on circularly polarized antennas fed with a microstrip transmission line does not include a systematic methodology to control and tune the reflection coefficient (S_{11}) and axial ratio (AR). To enable systematic tuning of those performance metrics, this study proposes a new, circularly polarized, circular microstrip patch antenna with truncated square slot. A combination of an edge-truncated square-slot and non-contacted electromagnetic coupling methods implemented in combination with circular patch results in a directional, left-handed circularly polarized (LHCP) pattern. This article discusses the analysis of several slot shapes that contribute to a good circularly polarized antenna. It also shows that the square slot with truncated edges is more effective in producing circular polarization than the conventional circular and usual square slot. Simulated and experimental results are in good agreement and indicate a −10-dB S_{11} and a 3-dB AR bandwidth of about 90 MHz and 25 MHz, respectively.

Index Terms─Antenna, circular patch, circular polarization, electromagnetically coupled feeding.

I. INTRODUCTION

In recent years, research on circularly polarized (CP) antennas has intensified due to their many advantages compared to linearly polarized antennas. This is due mainly to CP antennas' ability to operate with similar radiation performance despite being installed in various random orientations [1]. However, a CP antenna design is more complicated, since S_{11}, AR, and efficiency must be tuned simultaneously for satisfactory performance. Theoretically, a CP antenna can be produced when two orthogonal modes are excited with the same amplitude and 90° phase difference. Therefore, a rectangular-shaped patch usually is chosen, since it is easier to excite two orthogonal modes. In addition, the antenna shape can be structured to realize a circularly polarized antenna, as is the case in the Archimedean Spiral antenna [2]. Various methods have been presented to produce CP characteristics in rectangular-patch antennas. One example is reported in [3] where two methods are combined to enable CP. One of the most popular methods of implementing CP antennas is by truncating square patches fed by microstrip transmission lines (MTL), as in [4]. However, optimization needs to be performed carefully due to the multiple antenna parameters involved.

Note that using a 50-Ω probe feed is more flexible than an MTL implemented on the same surface. This is because a probe feed implemented using a coaxial connector can be positioned anywhere on the patch without affecting the main modal current distribution. Conventionally, an MTL easily can produce CP characteristics using the contacted feeding method, in which the MTL is connected directly to the patch. For circular polarization excitation, the MTL is located with an optimum offset from the center of the patch edges. Meanwhile, an MTL also can create CP characteristics by using a non-contacted method, in which the MTL is placed near the edges of the patch structure with the ideal gap between them.

One of the main challenges in enabling circular polarization for a circular-patch antenna is the unavailability of corners for orthogonal phase excitation. Several recent studies have investigated circular-shaped CP antennas [5-7]. In [5], several peripheral cuts are introduced at the

edge of the circular patch with optimum probe-feed to produce a CP antenna. In [6], good AR performance is obtained by introducing unbalanced circular slots on the radiating element. In addition, an unequal cross-shape on the ground plane with proper feeding point can function as a CP antenna, as reported in [7]. Unfortunately, these techniques are more complex due to the need for optimal slots or feed points.

In [8,9], a single MTL located closely beside the radiating element is used to produce an electromagnetically coupled feed. An optimal air gap produces a good CP antenna. This method is conventionally implemented for square-, meander- [8] and fractal-shaped ring [9] radiating elements. Corners available from these shapes facilitate excitation of the two orthogonal modes. However, existing literature does not discuss explicitly how to control and tune the S_{11} and AR [8,9] simultaneously. Modifying the antenna design affects both performance metrics, that is, impedance and AR bandwidth. Therefore, it is critical to know how the parameters of the antenna affect the S_{11} and AR.

In this investigation, a single, curved MTL is used to feed a circularly shaped patch antenna. To our best knowledge, this simple but novel technique has yet to be reported in open literature. The physical characteristics of the proposed antenna allow its AR and S_{11} to be tuned separately for operation in the 2.45 GHz industrial, medical and scientific (ISM) band. Before arriving at the final structure, several variations of the circular patch were investigated. The final antenna structure integrates a truncated square slot because of its capability to perform optimally as a CP antenna and its simplicity in tuning. Both simulation and measurement results show that the proposed antenna attains a satisfactory performance with a −10-dB impedance bandwidth of 90 MHz (2.41–2.50 GHz) and a 3-dB AR bandwidth of 25 MHz (2.433–2.458 GHz).

II. DESIGN APPROACH

Figure 1 depicts the basic circular microstrip-patch topology that was considered. The initial radius of the circular patch was obtained by using the procedure outlined in [10]. The antenna was fed by a 3-mm–wide transmission line, which matched to a 50-Ω SMA connector. Both antenna elements were implemented on an inexpensive 1.6-mm–thick FR4 substrate sized at WSub x LSub, with a relative permittivity (ε_r) of 4.5 and a loss tangent (tanδ) of 0.019. Simulations were performed using CST Microwave Studio, which is based on the finite integration technique (FIT). The time domain solver was used for numerical calculations, and the overall structure was divided into a maximum of 222,156 mesh cell. The 50-Ω port was excited by using a waveguide port.

Since it is well known that a properly excited circular patch generates circular polarization easily, it was chosen as the basis of this antenna. The curved 50-Ω MTL was used to feed power to the patch via electromagnetic

coupling. The start and end of the curved section were designed to enable excitation of two transverse modes with equal amplitudes and orthogonal phases, similar to a conventional patch, fed using a dual-feed, hybrid coupler.
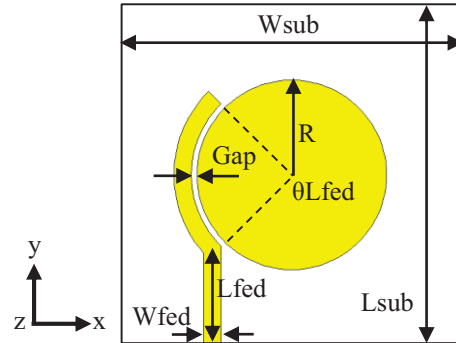

Fig. 1. Initial design of the proposed circular-patch antenna.

Figure 2 (a) shows the current distribution of the initial structure with the circular patch. It is observed that the current flows from the bottom corner of the circular patch around its perimeter. This structure was investigated further by adding a simple circular slot to form a ring. Figure 2 (b) shows this ring and the current distribution.
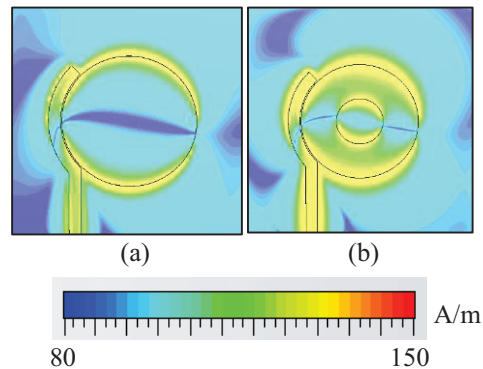

Fig. 2. Simulated current distribution at 2.45 GHz: (a) circular patch, and (b) circular ring.

It is evident that introducing a slot centered inside the radiator modifies the current distribution along the ring. This motivated further investigation of the circular-polarization characteristic. Parameterization of patch and slot sizes, which influence the S_{11} and AR simultaneously, increases the complexity in optimizing the circular-polarization characteristic when a circular ring slot is used. Therefore, the next section analyzes the slot shapes considered.

III. ANALYSIS OF PATCH SLOTS

This section describes the detailed analysis conducted on several slot shapes embedded within the circular patch. The analysis was performed with the objective of

identifying optimum slot shapes for satisfactory S_{11} and AR. Circular, square, and edge-truncated square slots were investigated.

First, analogous to [8], in which a square slot is embedded within a square patch, a circular slot embedded within a circular patch was investigated. Figure 3 (a) shows in a dashed box the circular slot centered within the circular patch antenna and its parameters. The radius of the circular patch is labeled R, and the radius of the circular slot is labeled Rs. Three different values of parameter Rs were examined, while R was fixed. Figures 3 (a) and 3 (b) show the S_{11} and AR when the circular slot was introduced to the patch antenna. Results show that the resonant frequency was slightly shifted with respect to the target resonance of 2.45 GHz when Rs was decreased (see Fig. 3 (a)), while its AR was above 10-dB (see Fig. 3 (b)). In contrast to the results in [8,9], in which ring shapes successfully enable circular polarization, it was concluded that the circular ring is not a good option to produce circular polarization for the proposed antenna.
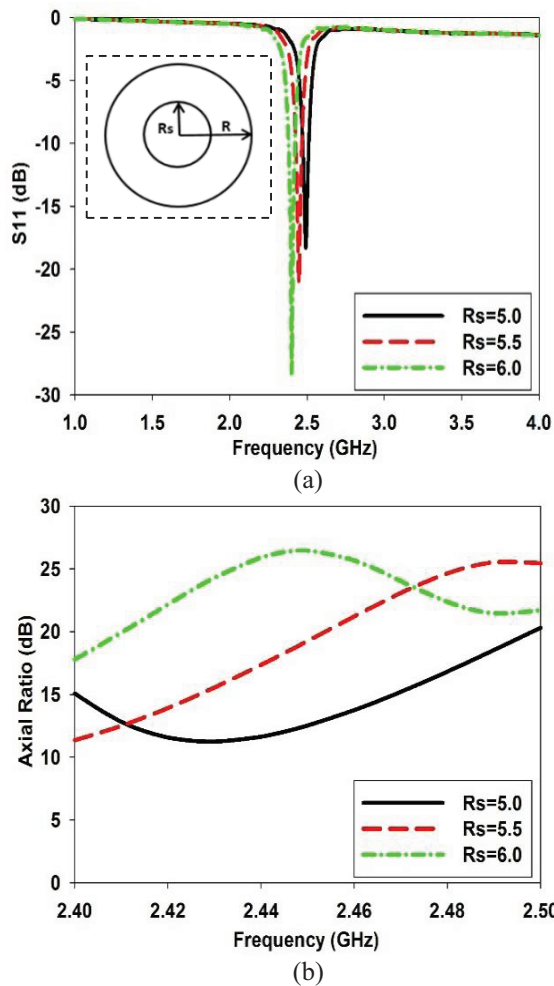
The next investigation concerned a square slot on the circular-patch antenna. The parameter S is the length of the square slot centered on the circular patch. Figure 4 shows the S_{11} and AR for this proposed structure. It can be seen that the resonance also is slightly shifted upward when the length of the square slot is decreased, as shown in Fig. 4 (a).

This characteristic also was observed in the previous structure. Thus, it can be concluded that the various slot shapes do not affect the S_{11} of this antenna significantly. However, the AR is highly affected by changes in the square-slot length. Figure 4 (b) indicates that an AR of less than 10-dB can be achieved. Its lowest point shifts upward when the value of S is decreased, similar to the behavior of S_{11}. Hence, this square-slot structure is more suitable to excite a circularly polarized characteristic on a regular circular-patch antenna. The same was observed in [8].
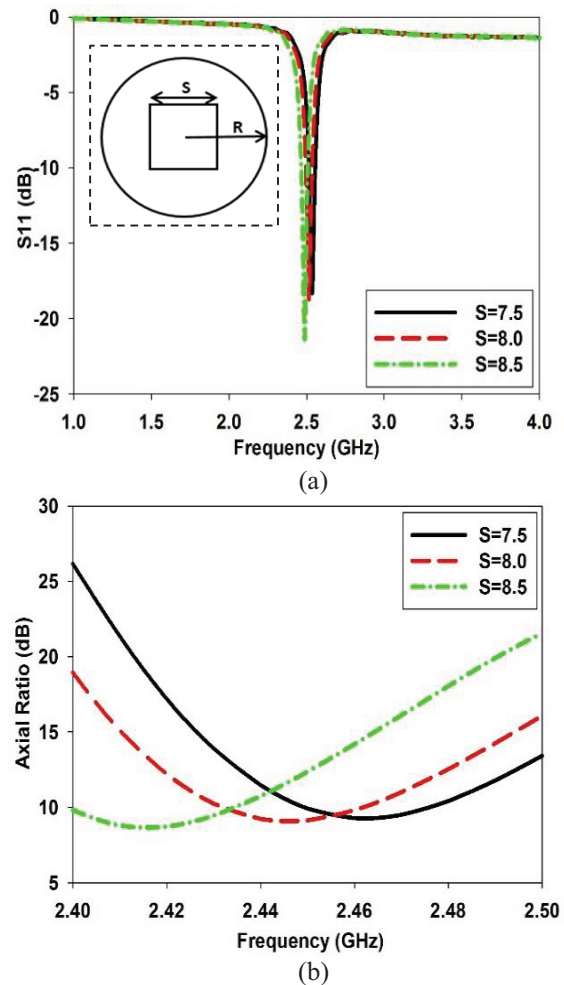

(a)

(b)

Fig. 4. Parametric study on the square slot: (a) reflection coefficient, and (b) axial ratio.

(a)

(b)

Fig. 3. Parametric study on the circular slot: (a) reflection coefficient, and (b) axial ratio.

By modifying the topology of the antenna in the

previous section, a truncated square slot with various truncation sizes was proposed and analyzed. In Fig. 5, the small dashed box shows the truncated square slot, with C representing its truncation length. A significant improvement of the AR was observed, while the S_{11} remained unchanged at 2.45 GHz, as shown in Fig. 5 (a). Therefore, it can be concluded that the truncation length, C, affects only the AR and not the resonant frequency, as evident in Fig. 5 (b). Consequently, the CP characteristic of the antenna is controllable via the truncation length and slot shape.
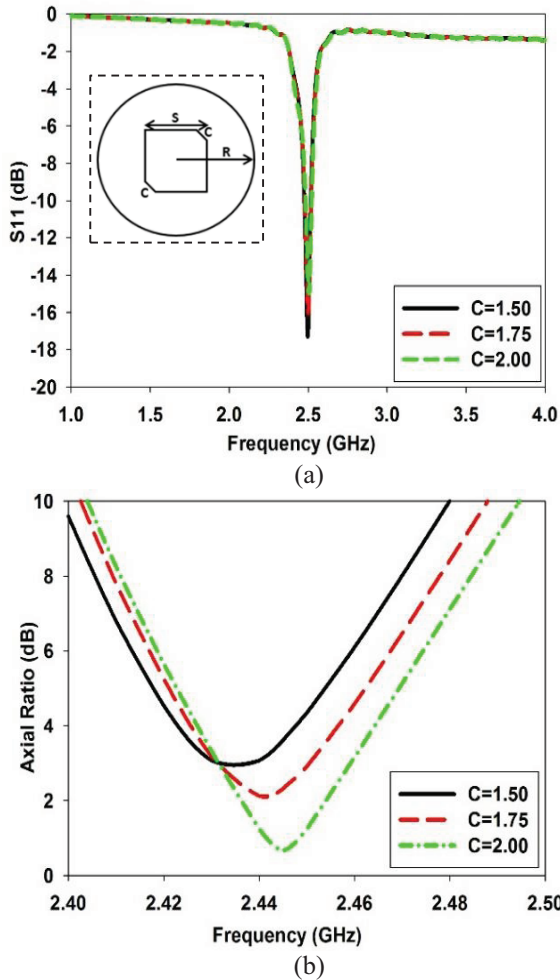

(a)

(b)

Fig. 5. Parametric study on the edge-truncated square slot: (a) reflection coefficient, and (b) axial ratio.

Because of its good AR, the truncated square slot was selected as the slot type to be integrated into the circular patch. The truncation length, C, can be adapted easily to tune the target AR; while the square-slot size, S, and radius of the patch, R, modify its S_{11}. Proper optimization of C excites two orthogonal modes similar in amplitude and 90° out of phase at 2.45 GHz. Then, this phase difference produces a good circularly polarized

antenna. Having identified the critical parameters, the final investigation was performed on the gap between the transmission line and patch, as it also influences antenna performance.

Figure 6 shows the parametric studies for several values of the gap between the transmission line and patch. Figure 6 (a) demonstrates the effect of several gap values on the S_{11}. Results show the S_{11} degrades to approximately −10-dB as the gap value is increased. This occurs because the intensity of the electromagnetic (EM) field coupled to the radiating element is decreased, along with a simultaneous decrease in power received by the patch element, causing degradation in the S_{11}. In addition, as Fig. 6 (b) shows, the AR is shifted to the higher frequencies, and its magnitude degrades as the gap increases. However, this degradation is not severe, and the values are maintained below 3-dB.
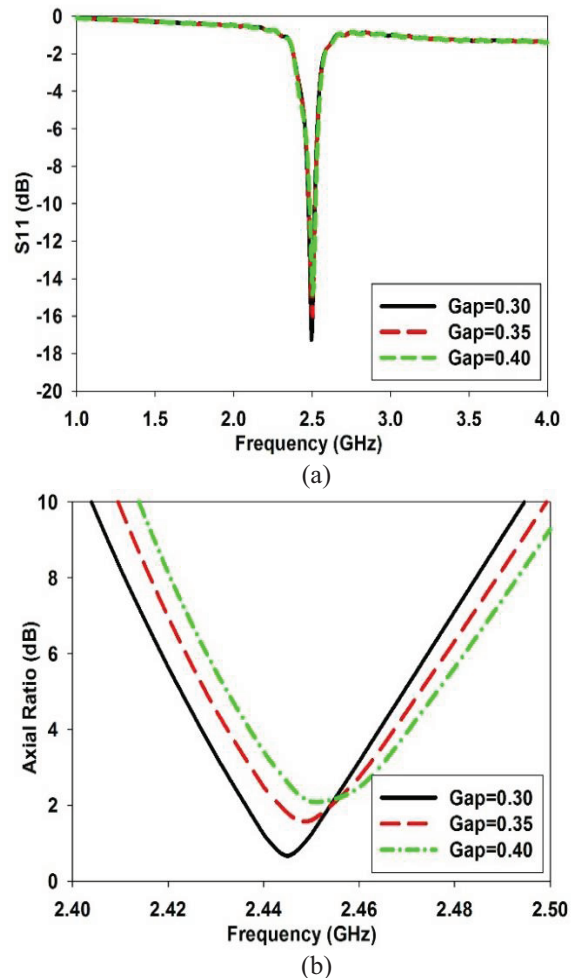

(a)

(b)

Fig. 6. Parametric study on the gap between transmission line and patch element: (a) reflection coefficient, and (b) axial ratio.

Figure 7 shows the simulated E-field distribution of

the edge-truncated structure. It is observed that the current flows circularly with left-handed CP, thus contributing to the left-hand circular-polarization radiation characteristic. The final step in the design process was to tune all parameters via simulations to optimize the antenna operation at 2.45 GHz in terms of S_{11}, AR, and gain. Table 1 summarizes the final dimensions of the proposed antenna. The overall dimension is $60 \times 60 \times 1.67$ mm^3.
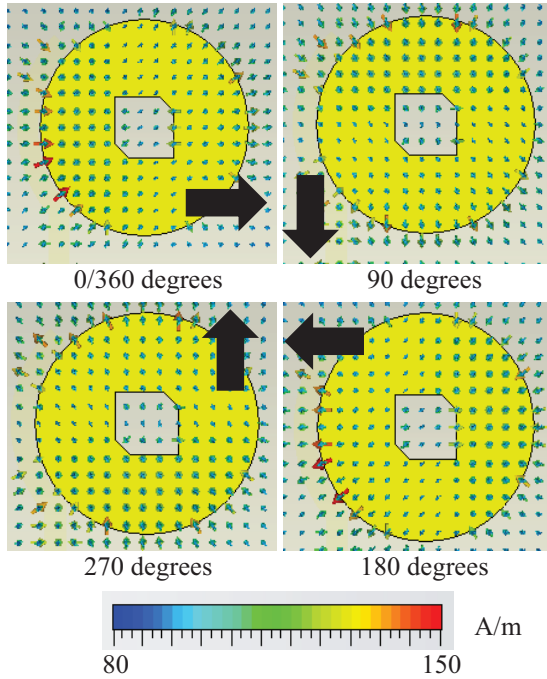

Fig. 7. Simulated current distribution of the edge-truncated square slot with different angles.

Table 1: Optimal dimensions of the proposed antenna (in mm)

Parameter	Value	Description
Wfed	2.98	Width of the MTL
Lfed	17.45	Length of the MTL
R	15.05	Affects S_{11}
S	8.52	Affects S_{11}
C	2.15	Affects to AR
Gap	0.35	Affects to AR

IV. RESULTS AND DICUSSION

Figure 8 shows the proposed antenna with the optimum value as fabricated after the simulation process. Its S_{11} performance is measured using a Rohde & Schwarz ZVL network analyzer.

Figure 9 shows the comparison between simulation and measurement. Results show good agreement between the measured and simulated S_{11}. The proposed antenna is excited at 2.45 GHz with -10-dB impedance bandwidth of 90 MHz (2.41–2.50 GHz). Maximum simulated S_{11} of

-17.32 and -13.73-dB were obtained for simulated and measured results, respectively.
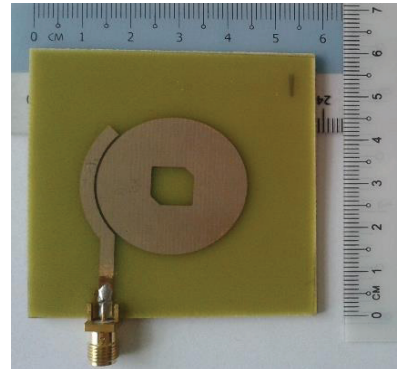
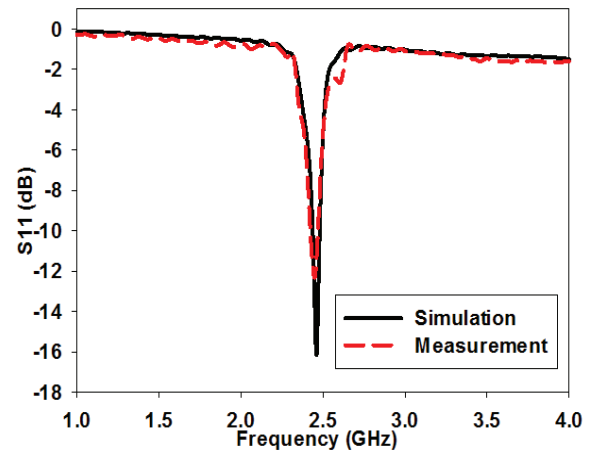

Fig. 8. Photograph of the prototyped antenna.

Fig. 9. Simulated and measured reflection coefficients.

Figure 10 shows the comparison between simulated and measured AR of the proposed antenna. The results show comparable agreement between measured and simulated values.

The minimum AR value from simulation is 0.33-dB, achieved at 2.45 GHz, and from measurement, 1.07-dB, achieved at 2.44 GHz. The simulated and measured 3-dB AR bandwidths are 34 MHz, or 1.39% (from 2.431–2.465 GHz), and 25 MHz, or 1.02% (from 2.433–2.458 GHz), respectively. Table 2 compares the proposed design to other single-band, single-layered, circular-patch antennas operating at 2.45 GHz using FR-4 substrate. It indicates that all antennas produced a narrow AR bandwidth, between approximately 1 and 1.5%.

From this investigation, it is clear that the proposed antenna topology enables simple AR tuning without altering S_{11} performance. In addition, it can be observed that the narrow impedance and AR bandwidths are due mainly to the fact that a single-layered topology was used. This narrow bandwidth characteristic is advantageous

for very specialized applications, such as wireless power transfer. A narrow impedance bandwidth and circular polarization enable efficient power transfer via reception of randomly polarized incident fields. For applications that require additional bandwidth, this structure can be improved further by adding additional substrate layers, at the cost of increased design complexity.
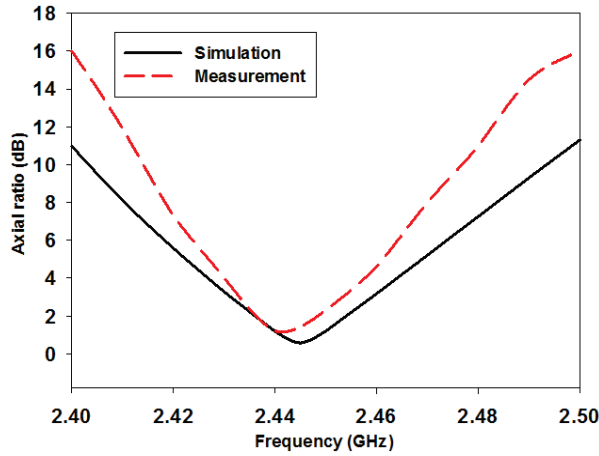

Fig. 10. Simulated and measured antenna axial ratio.

Table 2: Comparison of the 3-dB axial ratio bandwidth for a 2.45 GHz circular-patch antenna realized using FR-4 substrate

Ref.	AR BW		Ant Size	Feeding Technique
	MHz	%		
[5]	29	1.2	0.49λ	Contacted: coaxial
[6]	30	1.2	0.49λ	Contacted: coaxial
[7]	30	1.2	0.49λ	Contacted: coaxial
This work	25	1.0	0.49λ	Non-contacted: EM coupled

Figure 11 shows a comparison of the proposed antenna's simulated and measured right-hand circular polarization (RHCP) and left-hand circular polarization (LHCP) radiation patterns in the *xz*-plane and *yz*-plane. Simulations and measurements show good agreement. It can be seen that the proposed antenna radiates with a left-hand circular polarization in the upper half-space toward the +z-direction. Comparison between φ = 0° and 90° clearly shows that the RHCP magnitude is at least 15-dB below the LHCP in both *xz*- and *yz*-planes in the forward direction. The proposed antenna produces an almost symmetrical radiation pattern for 2.45 GHz and a maximum directivity of 6.528 dBi in the positive z-direction. At 2.45 GHz, the half-power beam width (HPBW) of the proposed antenna is about 94.2°. Figure 12 illustrates simulated and measured antenna radiation efficiency. The measured efficiency between 40% and 55% within the 2.4–2.5 GHz band is shifted slightly to higher frequencies compared to the simulated efficiency.

Nonetheless, it still is considered relatively high, making it suitable for either WLAN or rectenna applications.
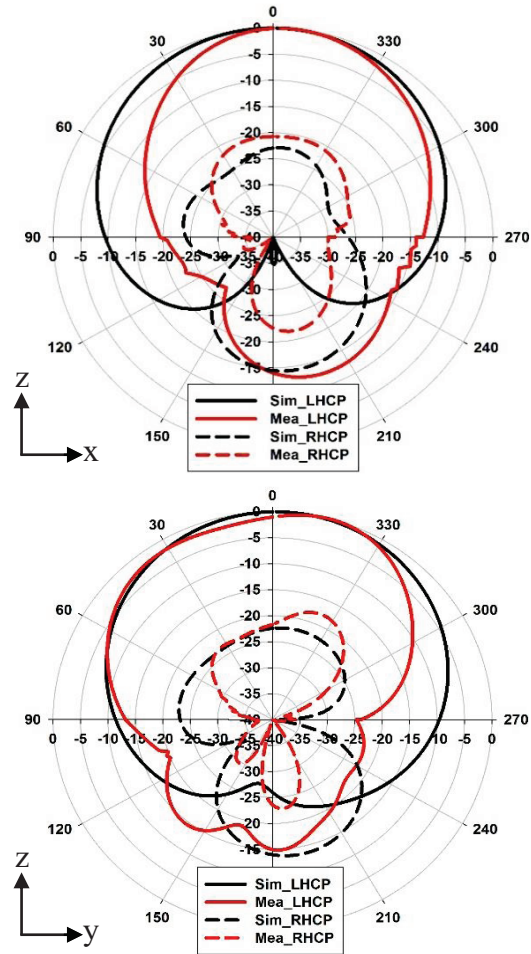

Fig. 11. Simulated and measured radiation pattern in the xz-plane and yz-plane at 2.45 GHz.
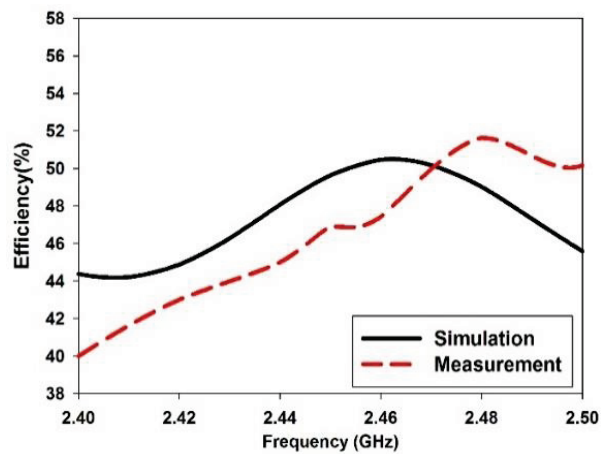

Fig. 12. Simulated and measured antenna radiation efficiency.

V. CONCLUSION

This work presents a novel, simple, low-cost circular-patch antenna with circular-polarization capability that enables controllable tuning of AR and S_{11}. The proposed antenna consists of a patch integrated with a truncated square slot and is electromagnetically coupled to a single microstrip transmission line for operation in the 2.45 GHz ISM band. Circular-polarization behavior is enabled via a truncated rectangular slot and is easily tunable without affecting the overall structure's impedance matching. The antenna attains satisfactory performance, with a −10-dB impedance bandwidth of 90 MHz (2.41–2.50 GHz) and a 25-MHz (2.433–2.458 GHz) 3-dB AR bandwidth.

ACKNOWLEDGMENTS

REFERENCES

[1] Q. Liu, Y. Liu, Y. Wu, M. Su, and J. Shen, "Compact wideband circularly polarized patch antenna for CNSS applications," *IEEE, Antennas and Wireless Propagation Letters*, vol. 12, pp. 1280-1283, 2013.

[2] O. A. Mashaal, S. K. A. Rahim, A. Y. Abdulrahman, M. I. Sabran, M. S. A. Rani, and P. S. Hall, "A coplanar waveguide fed two arm archimedean spiral slot antenna with improved bandwidth," *IEEE Transactions on Antennas and Propagation*, vol. 61, no. 2, pp. 939-943, Feb. 2013.

[3] M. I. Sabran, S. K. A. Rahim, M. S. A. Rani, and M. Z. M. Nor, "A single band dual-fed circular polarization microstrip antenna for RFID application," *2011 IEEE International RF and Microwave Conference (RFM)*, Seremban, Negeri Sembilan Malaysia, pp. 137-140, Dec. 12-14, 2011.

[4] S. M. Noghabaei, S. K. A. Rahim, P. J. Soh, M. Abedian, and G. A. E. Vandenbosch, "A dual-band circularly-polarized patch antenna with a novel asymmetric slot for WiMAX application," *Radioengineering*, vol. 22, no. 1, 2013.

[5] F. J. Huang, T. C. Yo, C. M. Lee, and C. H. Luo, "Design of circular polarization antenna with harmonic suppression for rectenna application," *IEEE Antennas and Wireless Propagation Letters*, vol. 11, pp. 592-595, 2012.

[6] T. C. Yo, C. M. Lee, C. M. Hsu, and C. H. Luo, "Compact circularly polarized rectenna with unbalanced circular slots," *IEEE Transactions on Antennas and Propagation*, vol. 56, no. 3, pp. 882-886, Mar. 2008.

[7] W. S. Yoon, D. H. Lee, K. J. Lee, S. H. Kim, S. M. Han, and Y. S. Kim, "A circular patch antenna for a switchable circular polarization sense with a slotted ground structure," *Antennas & Propagation Conference, 2009. LAPC 2009*, Loughborough, pp. 309-312, Nov. 16-17, 2009.

[8] J. Choi, S. Pyo, S. M. Han, and Y. S. Kim, "Circularly polarized microstrip antennas using single-fed EM coupled ring resonators," *International Symposium on Antenna and Propagation (ISAP)*, Bangkok, Thailand, Oct. 20-23, 2009.

[9] M. A. M. Yusop, M. K. A. Rahim, M. F. Ismail, and A. Wahid, "Circular polarization fractal koch microstrip patch antenna using single-fed EM coupled ring resonators," *2010 IEEE Asia-Pacific Conference on Applied Electromagnetics (APACE)*, Port Dickson, Malaysia, pp. 1-4, Nov. 9-11, 2010.

[10] C. A. Balanis, *Antenna Theory: Analysis and Design*, 2nd ed., Hoboken, NJ, John Wiley & Son, 1997.

Mursyidul Idzam Sabran was born in Selangor, Malaysia He obtained his degree in Electrical Engineering (Telecommunication) in 2009 and M.Sc. in Master of Engineering (Electrical) in 2012 from UTM Skudai, Johor Malaysia. He is currently a full-time Ph.D. Research Student at the Wireless Communication Centre (WCC), Faculty of Electrical Engineering, Universiti Teknologi Malaysia (UTM), Johor, Malaysia.

Sharul Kamal Abdul Rahim received his first degree from University of Tennessee, USA majoring in Electrical Engineering, graduating in 1996, M.Sc. in Engineering (Communication Engineering) from Universiti Teknologi Malaysia (UTM) in 2001, and Ph.D. in Wireless Communication System from University of Birmingham, UK in 2007. Currently, he is an Associate Professor at Wireless Communication Centre, Faculty of Electrical Engineering, UTM. His research interest is Smart Antenna on Communication System.

Ping Jack Soh was born in Sabah, Malaysia. He received the Bachelor and Master degrees in Electrical Engineering (Telecommunication) from Universiti Teknologi Malaysia (UTM) in 2002 and 2005, respectively, and the Ph.D. degree in Electrical Engineering from KU Leuven, Belgium in 2013. He is currently a Senior Lecturer at the

School of Computer and Communication Engineering, Universiti Malaysia Perlis (UniMAP) and the Deputy Dean of the University's Research Management and Innovation Center (RMIC). Soh was the recipient of the IEEE Antennas and Propagation Society (AP-S) Doctoral Research Award in 2012, the IEEE Microwave Theory and Techniques Society (MTT-S) Graduate Fellowship for Medical Applications in 2013 and the International Union of Radio Science (URSI) Young Scientist Award in 2015. He was also the second place winner of the IEEE Presidents' Change the World Competition and IEEE MTT-S Video Competition, both in 2013, besides being awarded the Computer Simulation Technology (CST) University Publication Award in 2011 and 2012.

Chee Yen Leow obtained his B.Eng. degree in Computer Engineering from Universiti Teknologi Malaysia (UTM) in 2007. Since July 2007, he has been an Academic Staff in the Faculty of Electrical Engineering, UTM. In 2011, he obtained a Ph.D. degree from Imperial College London. He is currently a Senior Lecturer in the faculty and a Member of the Wireless Communication Centre (WCC), UTM.

Guy A. E. Vandenbosch received the M.S. and Ph.D. degrees in Electrical Engineering from the Katholieke Universiteit Leuven, Leuven, Belgium, in 1985 and 1991, respectively. From 1991 to 1993, he held a Postdoctoral Research Position at the Katholieke Universiteit Leuven. Since 1993, he has been a Lecturer, and since 2005, a Full Professor at the same university.

His research interests are in the area of electromagnetic theory, computational electromagnetics, planar antennas and circuits, nano-electromagnetics, EM radiation, EMC, and bio-electromagnetics. His work has been published in ca. 220 papers in international journals and has been presented in ca. 300 papers at international conferences. Vandenbosch has convened and chaired numerous sessions at many conferences. He was co-chair and vice-chair of the European Microwave Week in Amsterdam in 2004 and 2012, respectively. In 2004, he chaired the TPC of the European Microwave Conference within this Week. He was a Member of the TPC of the European Microwave Conference in 2005, 2006, 2007, and 2008. He was one of the vice chairs within the team organizing the EuCAP conference 2014 in The Hague, The Netherlands.